

ARM

CLIMATE RESEARCH FACILITY

Microwave Radiometer – 3 Channel (MWR3C) HANDBOOK



May 2012



U.S. DEPARTMENT OF
ENERGY

Office of
Science

Work Supported by the U.S. Department of Energy
Office of Science, Office of Biological and Environmental Research

DISCLAIMER

This report was prepared as an account of work sponsored by the U.S. Government. Neither the United States nor any agency thereof, nor any of their employees, makes any warranty, express or implied, or assumes any legal liability or responsibility for the accuracy, completeness, or usefulness of any information, apparatus, product, or process disclosed, or represents that its use would not infringe privately owned rights. Reference herein to any specific commercial product, process, or service by trade name, trademark, manufacturer, or otherwise, does not necessarily constitute or imply its endorsement, recommendation, or favoring by the U.S. Government or any agency thereof. The views and opinions of authors expressed herein do not necessarily state or reflect those of the U.S. Government or any agency thereof.

Microwave Radiometer – 3 Channel (MWR3C) Handbook

MP Cadeddu

May 2012

Work supported by the U.S. Department of Energy,
Office of Science, Office of Biological and Environmental Research

Contents

1.0	General Overview	1
2.0	Contacts	1
2.1	Mentor	1
2.2	Vendor/Instrument Developer	1
3.0	Deployment Locations and History	1
4.0	Near-Real-Time Data Plots	1
5.0	Data Description and Examples	2
5.1	Data File Contents	2
5.1.1	Primary Variables and Expected Uncertainty	2
5.1.2	Secondary/Underlying Variables	2
5.1.3	Diagnostic Variables	3
5.1.4	Data Quality Flags.....	3
5.1.5	Dimension Variables	5
5.2	Annotated Examples	5
5.3	User Notes and Known Problems	6
5.4	Frequently Asked Questions	6
6.0	Data Quality.....	7
6.1	Data Quality Health and Status	7
6.2	Data Reviews by Instrument Mentor.....	7
6.3	Data Assessments by Site Scientist/Data Quality Office	7
6.4	Value-Added Products	7
7.0	Instrument Details.....	7
7.1	Detailed Description.....	7
7.1.1	List of Components	8
7.1.2	System Configuration and Measurement Methods	8
7.1.3	Specifications	9
7.2	Theory of Operation	9
7.3	Calibration.....	10
7.3.1	Theory	10
7.3.2	Procedures	10
7.3.3	History	12
7.4	Operation and Maintenance	12
7.4.1	User Manual	12
7.4.2	Routine and Corrective Maintenance Documentation	12
7.4.3	Software Documentation.....	12
7.4.4	Additional Documentation	12

7.5 Glossary..... 12

8.0 References 13

Figures

Figure 1. Brightness temperatures measured by the MWR3C at 23.834 and 30 GHz (black and red) versus MWR measurements at 23.8 and 31 GHz (y-axis).....	5
Figure 2. Three rain events in Gan, Maldives, and the effect of the rain mitigation system on the MWR (violet line, 31.4 GHz) and the MWR3C (black line, 30 GHz).	6
Figure 3. Left panel: comparison of PWV retrievals from the MWR3C physical (x-axis) and neural network (y-axis) retrievals [1]..	9
Figure 4. Left panel: Percentage PWV error as a function of PWV from various instruments and algorithms	10
Figure 5. Instantaneous T_{nd} values derived from tip curves (brown points) and running median values (black line).....	12

Tables

Table 1. Status and location of the MWRHF.....	1
Table 2. Primary variables	2
Table 3. Secondary variables	2
Table 4. Diagnostic variables.....	3
Table 5. Data quality thresholds	4
Table 6. Dimension Variables.....	5
Table 7. Instrument specifications	9

1.0 General Overview

The microwave radiometer 3-channel (MWR3C) provides time-series measurements of brightness temperatures from three channels centered at 23.834, 30, and 89 GHz. These three channels are sensitive to the presence of liquid water and precipitable water vapor.

2.0 Contacts

2.1 Mentor

Maria Cadeddu
 Environmental Sciences Division
 Argonne National Laboratory, Bldg. 240
 Argonne, Illinois, 60439
 Phone: (630) 252-7408
 Email: mcadeddu@anl.gov

2.2 Vendor/Instrument Developer

Radiometrics Corporation
 2840 Wilderness Place Unit G
 Boulder, CO 80301-5414
 Phone: (303) 449-9192
info@radiometrics.com

3.0 Deployment Locations and History

Table 1. Status and location of the MWR3C.

Serial Number	Property Number	Location	Date Installed	Date Removed	Status
13		SGP C1	10/01/2011	N/A	Operational
11		AMF2	01/11/2011	N/A	Operational
10		TWP C3	12/01/2011	N/A	Operational

4.0 Near-Real-Time Data Plots

Plots of near-real-time data can be viewed at the DQ Explorer system accessible through <http://dq.arm.gov/>. Select the desired site and datastream. The MWR3C datastream is “sssmwr3cFF.b1” where ‘sss’ is the site (SGP, TWP, etc.) and ‘FF’ is the facility (C1, M1, etc.)

5.0 Data Description and Examples

5.1 Data File Contents

Datastreams available from the ARM Data Archive are named sssmwr3cFF.b1 and contain calibrated brightness temperatures and retrievals. Raw data files are available upon request, and they are named sssmwr3cFF.00.yyyymmdd.hhmmss.raw.PR-2289C-SN_yyyy-mm-dd_hh-mm-ss.csv. Data files containing the calibration results from tip curves are named sssmwr3cFF.00.yyyymmdd.hhmmss.raw.PR-2289C-SN_yyyy-mm-dd_hh-mm-ss_dailytips.csv.

5.1.1 Primary Variables and Expected Uncertainty

The primary variables measured by the MWR3C are brightness temperatures at 23.834, 30, and 89 GHz. By relating the observed radiances to atmospheric water vapor and liquid water, it is possible to derive precipitable water vapor (PWV) and liquid water path (LWP) from the measurements. Retrievals of integrated water vapor and liquid water path obtained from brightness temperatures measured at the three frequencies are provided in the data files. Uncertainties in the retrieved PWV and LWP are provided in the data files as individual error bars.

Table 2. Primary variables.

Variable Name	Quantity Measured	Unit	Uncertainty (1 σ)
Tbsky23	23.834 GHz sky brightness temperature	K	0.5 K
Tbsky30	30 GHz sky brightness temperature	K	0.5 K
Tbsky89	89 GHz sky brightness temperature	K	1.5 K
lwp	Liquid water path	mm	~0.015 mm
pwv	Precipitable water vapor	cm	~0.05 cm

5.1.2 Secondary/Underlying Variables

Table 3. Secondary variables.

Variable Name	Quantity Measured	Unit	Uncertainty (1 σ)
Time	Time offset from midnight	s	
surface_temperature	Ambient temperature	C	0.5
surface_pressure	Pressure	KPa	0.1
surface_relative_humidity	Relative humidity	%	5
wind_direction_avg	Average wind direction	deg	3
wind_direction_max	Wind direction maximum	deg	3
wind_direction_min	Wind direction minimum	deg	3
wind_speed_avg	Average wind speed	m/s	5%
wind_speed_max	Wind speed maximum	m/s	5%
wind_speed_min	Wind speed minimum	m/s	5%
infrared_temperature	Zenith-pointing infrared temperature at 10 μ m	K	0.5
rain_accumulation	Rain accumulation	mm	5%
rain_duration	Rain duration	s	10
rain_intensity	Rain intensity	mm/hr	Not provided

Table 3 (contd)			
Variable Name	Quantity Measured	Unit	Uncertainty (1 σ)
hail_accumulation	Hail accumulation	hit/cm ²	Not provided
hail_duration	Hail duration	s	10
hail_intensity	Hail intensity	hit/(hr cm ²)	Not provided
rain_peak_intensity	Rain peak intensity	mm/hr	Not provided

5.1.3 Diagnostic Variables

The following diagnostic variables are in the PR-2289C-SN_yyyy-mm-dd_hh-mm-ss_dailytips.csv files associated with the raw datastream.

Table 4. Diagnostic variables.

Variable Name	Quantity Measured	Unit	Uncertainty (1 σ)
TcaseK	Physical temperature of the K-band receiver case	K	5 K
TloadK	Physical temperature of the K-band radiometer reference load	K	5 K
TcaseW	Physical temperature of the W-band receiver case	K	1.5 K
TloadW	Physical temperature of the W-band radiometer reference load	K	2.5 K
Tnd23834	Instantaneous Tnd at 23.834 GHz from tip curves	K	0.5 K
Tnd(0C)23834	Instantaneous Tnd at 23.834 GHz at nominal temperature	K	0.5 K
TndTC23834	Temperature correction coefficient at 23.834 GHz	K/K	
Tmr23834	Mean radiating temperature at 23.834 GHz	K	10 K
R23834	Tip curve correlation coefficient		
Tnd30000	Instantaneous Tnd at 30.000 GHz from tip curves	K	0.5 K
Tnd(0C)30000	Instantaneous Tnd at 30.000 GHz at nominal temperature	K	0.5 K
TndTC30000	Temperature correction coefficient at 30.000 GHz	K/K	
Tmr30000	Mean radiating temperature at 30.000 GHz	K	10 K
R300000	Tip curve correlation coefficient		
Tnd89000	Instantaneous Tnd at 89.000 GHz from tip curves	K	2 K
Tnd(0C)89000	Instantaneous Tnd at 89.000 GHz at nominal temperature	K	2 K
TndTC89000	Temperature correction coefficient at 89.000 GHz	K/K	
Tmr89000	Mean radiating temperature at 89.000 GHz	K	10 K
R89000	Tip curve correlation coefficient		

5.1.4 Data Quality Flags

Data quality flags are named qc_‘fieldname’ (i.e. qc_tbsky90). Possible values for qc_flags are:

- 0 (value is within the specified range)
- 1 (missing value)
- 2 (value is less than the specified minimum)

- 4 (value is greater than the specified maximum)
- 8 (value failed the valid “delta” check).

Specified maximum and minimum values are shown in Table 5.

Table 5. Data quality thresholds.

Field Name	Min	Max
Tbsky23	2.73	330
Tbsky30	2.73	330
Tbsky89	2.73	330
surface_temperature	-50	50
surface_pressure	70	110
surface_relative_humidity	0	110
wind_direction_avg	0	360
wind_direction_max	0	360
wind_direction_min	0	360
wind_speed_avg	0	30
wind_speed_max	0	30
wind_speed_min	0	30
infrared_temperature	173	305
rain_accumulation	0	30
rain_duration	0	21600
rain_intensity	0	500
hail_accumulation	0	10
hail_duration	0	3600
hail_intensity	0	500
rain_peak_intensity	0	30

5.1.5 Dimension Variables

Table 6. Dimension variables.

Field Name	Quantity	Unit
base_time	Base time in Epoch	seconds since 1970-1-1 0:00:00 0:00
time_offset	Time offset from base_time	s
Lat	north latitude	degrees
Lon	east longitude	degrees
Alt	altitude	meters above Mean Sea Level

5.2 Annotated Examples

In this section are some examples of data. Figure 1 [1] shows a comparison of brightness temperatures between the MWR and the MWR3C at the SGP site for the month of November 2011. The figure shows a very good consistency of the measurements from the two instruments. For example, the root mean square differences between measured and modeled brightness temperatures (green points) are 0.7 K and 0.4 K for the 23.834 and 30 GHz respectively. The slightly higher RMS differences in the 23.834 GHz channel may be due to a residual temperature dependence of the calibration of that channel.

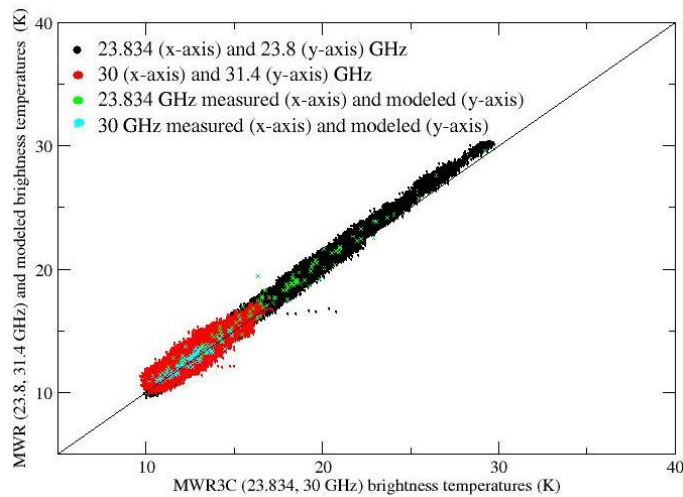


Figure 1. Brightness temperatures measured by the MWR3C at 23.834 and 30 GHz (black and red) versus MWR measurements at 23.8 and 31 GHz (y-axis). Green and cyan points are brightness temperatures at 23.834 and 30 GHz measured by the MWR3C (x-axis) and modeled (y-axis). Data were collected at the SGP during the month of November 2011. Figure from [1].

The rain mitigation system is designed to keep the two receivers’ lenses dry in situations of high humidity or light rain. For this purpose a stream of warm air is blown across the lenses when the relative humidity

exceeds a user-adjustable threshold. Air is blown at high speed during rain to keep the lenses clear of standing water. The rain detection and mitigation system of the MWR3C shows improved capability in quickly drying the lenses after a rain event as shown in Figure 2 [1]. The three panels show brightness temperatures (30 GHz) during three rain events in Gan, Maldives, in December 2011. Red crosses indicate rain rate (mm/hr) as reported by the MWR3C rain sensor. Pink crosses indicate the times when the MWR rain flag was on (100) and off (0). During these times the heater in the MWR dew blower was blowing warm air on the radiometer's Teflon window. The two black lines with arrows start when the rain stops (according to the MWR3C sensor). In general the MWR3C brightness temperatures drop back to normal levels after approximately 5–10 minutes from the end of the rain, suggesting that this is the time necessary to completely free the lens of standing water.

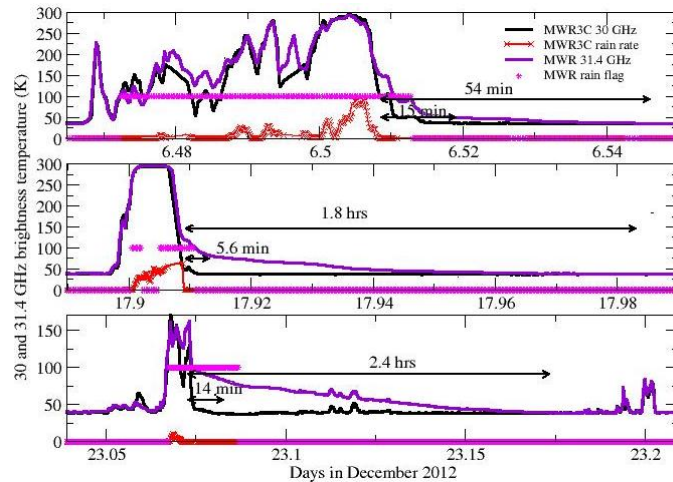


Figure 2. Three rain events in Gan, Maldives, and the effect of the rain mitigation system on the MWR (violet line, 31.4 GHz) and the MWR3C (black line, 30 GHz). Red points are the rain rate (mm/hr) measured by the MWR3C weather station; pink points represent the times when the MWR rain flag was on. The black solid lines indicate the time between the end of the rain (zero rain rate according to the MWR3C) and the return of brightness temperatures to approximate pre-rain values. Figure from [1].

5.3 User Notes and Known Problems

This section is not yet available.

5.4 Frequently Asked Questions

This section is not yet available.

6.0 Data Quality

6.1 Data Quality Health and Status

Daily quality check on this data stream can be found at the DQ Explorer page: <http://dq.arm.gov/>. Select the desired site and datastream. For example, for the MWR3C located at the site “SGP”, the datastream is “sgpmwr3cC1.b1” and the facility is “C1”.

6.2 Data Reviews by Instrument Mentor

The instrument mentor submits a monthly summary report accessible from the instrument web page. Some of the general checks performed by the instrument mentor are shown below.

1. In general, the brightness temperature time series should be smooth and with low noise levels.
2. Brightness temperatures should be greater than 2.75 K and less than approximately 330 K.
3. External temperature readings can be compared to tower measurements. The agreement should be +/- 2 K.
4. External pressure readings can be compared to tower measurements. The agreement should be +/- 5 KPa.
5. External relative humidity readings can be compared to tower measurements. The agreement should be +/- 5%
6. Measured brightness temperatures are also compared with model computations as a general quality check.
7. Data from the rain detection system are routinely checked against other similar measurements depending on their availability at a given site.

6.3 Data Assessments by Site Scientist/Data Quality Office

The Data Quality office daily data assessment can be viewed at the DQ Explorer web page.

6.4 Value-Added Products

The MWRRET algorithm provides physical retrievals of water vapor and liquid water path.

7.0 Instrument Details

7.1 Detailed Description

The MWR3C measures sky radiances at three frequencies: 23.834, 30, and 89 GHz. Radiance measurements are converted to “equivalent brightness temperatures” through the calibration procedure. Below is detailed description of the instrument components.

7.1.1 List of Components

RF section: two microwave receivers PR2289 model manufactured by Radiometrics Corp.

- FLIR DP300 pan tilt unit
- Main Junction box
- Embedded PC computer controller
- Radiometer stand
- Rain Effect Mitigation (REM) system composed of a blower assembly and two heaters
- Vaisala weather station WXT510
- Garmin GPS unit
- Heitronix KT15II infrared thermometer

7.1.2 System Configuration and Measurement Methods

In this section we give a brief description of the MWR3C hardware configuration. The MWR3C is composed of two PR-series microwave receivers. The PR2230 is the K-band receiver and can be calibrated to up to 30 frequencies between 22 and 30 GHz. In operational mode only two channels (22.834 and 30 GHz) are calibrated. The K-band channels have a bandwidth of 300 MHz. The PR8900 is the W-band receiver that is calibrated at 89 GHz (1.9 GHz bandwidth). The receivers are enclosed in a watertight case equipped with active moisture and pressure control. The entire receiver subsystem is thermally stabilized to 30 mK, with the exception of the external lens. Residual temperature dependences due to the external lens are corrected in the calibration procedure with the use of additional temperature coefficients. The radiation entering the lens passes through a feedhorn and is directed to a PIN switch. The switch is periodically set to a load position. In this case the receiver sees the “black body” that is kept at a temperature carefully monitored with a precision thermometer. The gain is monitored by periodically injecting a calibrated noise through a noise diode. The receivers are moved in azimuth and elevation by a pan tilt unit, and they are equipped with internal accelerometers to precisely determine the elevation angle. In normal operation mode the radiometers observe the sky in zenith position. Zenith measurements are interrupted approximately every 15 minutes to collect scanning measurements used to perform the absolute calibration. All data processing and software operations are performed by an embedded computer located inside the Main Junction Box.

The two receivers’ lenses are kept free of dew and water drops in drizzle conditions by the Rain Effect Mitigation (REM) System. The system is composed of a dewblower and two heaters that blow warm air on the lenses when the relative humidity exceeds a user-selectable threshold.

7.1.3 Specifications

Table 7. Instrument specifications.

Parameter	Value
Receiver noise temperature 23.834 GHz	< 500 K
Receiver noise temperature 30 GHz	< 500 K
Receiver noise temperature 89 GHz	<1100
Channel bandwidth K-band	300 MHz
Channel bandwidth W-band	1900 MHz
Radiometric resolution	0.4 K RMS@1 s integration time
Receiver and antenna thermal stabilization	< 30 mK (excluded external lens)
Integration time	>=1 s
HPBW K band channels	~3.0°
HPBW W band channel	~3.5°
Temperature range	-40 to +45 C (Environmental Chamber tested)

7.2 Theory of Operation

The three channels of the MWR3C are highly sensitive to the presence of water vapor and liquid water in the atmosphere. The two K-band frequencies (23.834 and 30 GHz) are similar to the frequencies sampled by the MWR (23.8 and 31.4 GHz) to ensure continuity of the measurements. The additional 89-GHz channel provides increased sensitivity to the presence of cloud liquid water. The additional channel should therefore improve LWP retrievals, particularly when the liquid water amount is low. Real-time retrievals of integrated water vapor and liquid water path are available from the ARM Data Archive in the datastream sssmwr3cFF.b1. The retrievals are obtained with a neural network algorithm similar to the one described in [2]. Physical retrievals are available as VAPs. In Figure 3 (left panel, [1]) we show a comparison of PWV retrieved with the neural network and the physical retrieval at the SGP and at the Gan Island deployment of the ARM Mobile Facility 2 (AMF2). In the right panel LWP retrievals are shown.

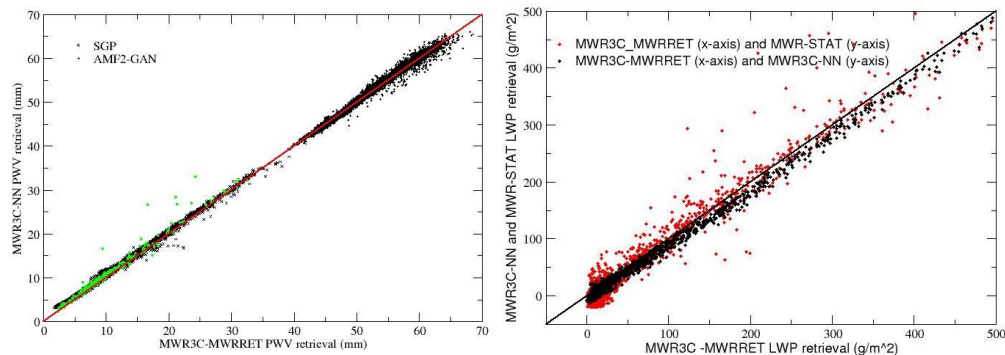


Figure 3. Left panel: comparison of PWV retrievals from the MWR3C physical (x-axis) and neural network (y-axis) retrievals [1]. At the SGP (crosses) and AMF2-GAN (circles). Green points represent radiosonde measurements. Right panel: LWP retrievals from the MWR3C physical (x-axis) and neural network (y-axis, black) retrievals. Red points are the MWR statistical retrievals.

With the addition of the 89-GHz channel, the PWV and LWP retrieval uncertainty can be reduced as shown in Figure 4 [1].

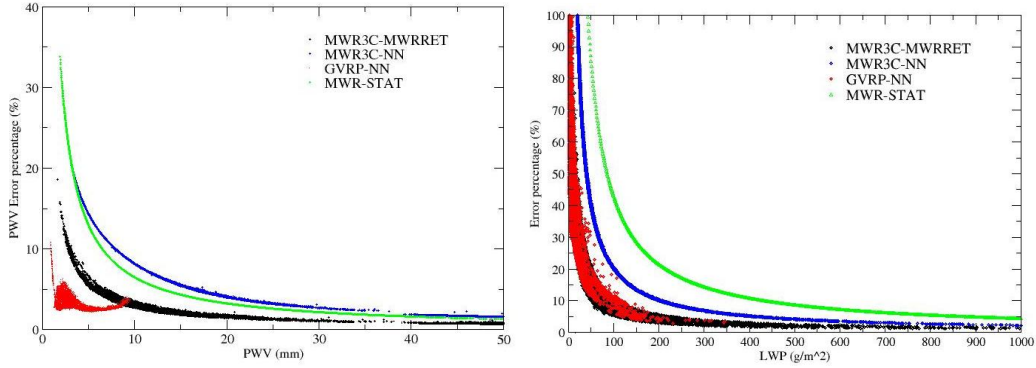


Figure 4. Left panel: Percentage PWV error as a function of PWV from various instruments and algorithms. Right panel: same as in the left panel but for LWP retrieval. Figure from [1].

7.3 Calibration

7.3.1 Theory

Once in the field, the MWR3C calibrates exclusively with tip curves. In-factory calibration determines the receiver non-linearity coefficients and the lens temperature-dependent offset. A residual temperature dependence of the lens is derived from the tip curves results. With the tip curve algorithm, the gain and receiver temperature are uniquely determined. The processing of the tip curves is designed to be consistent with the MWR's [3] and MWRHF's [1] calibration procedures. Tip curves are collected every 15 minutes. In the tip curve procedure, a linear regression is performed between the optical thickness and the air mass. The straight line is extrapolated to zero air mass. The detector reading at this point corresponds to a radiometric temperature, which equals the system noise temperature plus 2.7 K. A second detector voltage is measured with the radiometer pointing at the ambient temperature with known radiometric temperature. Various corrections are applied to achieve increased accuracy in the results. Once a sufficiently large number of acceptable tip curves are collected (the number of points as well as the acceptance criterion are user-selectable), they are processed, and a median value is used in the computations of brightness temperatures.

7.3.2 Procedures

The calibration algorithm is based on the assumption that although noise diodes are known to be stable over time, the effective noise diode injection temperature as determined from tip curves will eventually show some drift over a period of a few months. The radiometer equations used to calibrate the brightness temperatures are the following:

$$V_{load} = g(T_{rcv} + T_{load} + Offset)^\alpha \quad (1)$$

$$V_{loadND} = g(T_{rcv} + T_{load} + Offset + T_{ND})^\alpha \quad (2)$$

$$V_{sky} = g(T_{rcv} + T_{sky})^\alpha \quad (3)$$

Where V_{load} and V_{loadND} are detector voltages recorded when viewing the internal reference load with the noise diode off and on and V_{sky} are voltages recorded when viewing the sky. The noise diode injection temperature T_{ND} and the *Offset* have a residual temperature dependence:

$$T_{ND} = T_{ND}^0 + c_1 T_c \quad (4)$$

$$Offset = Offset^0 - c_2 T_c \quad (5)$$

Where T_{ND}^0 and $Offset^0$ are the values at the nominal temperature of 0° C, c_1 and c_2 are coefficients, and T_c is the physical temperature of the receiver case expressed in degrees Celsius. The gain is therefore expressed as:

$$g = \left(\frac{V_{loadND}^{1/\alpha} - V_{load}^{1/\alpha}}{T_{ND}} \right)^\alpha, \quad (6)$$

and the receiver temperature T_{rcv} as:

$$T_{rcv} = \left(\frac{V_{load}}{g} \right)^\alpha - T_{load} - Offset. \quad (7)$$

The sky temperature is computed as:

$$T_{sky} = \left(\frac{V_{sky}}{g} \right)^{1/\alpha} - T_{rcv} \quad (8)$$

Eq. 8 is the basic equation that is used in the calibration. The gain is monitored at each measurement point. On the other hand, the noise diode is calibrated with the tip curves procedure. During tip calibrations, the radiometer scans on both sides of the window and also acquires readings of the internal load. The noise diode is calibrated with the following equation:

$$T_{ND} = \left(\frac{V_{loadND}^{1/\alpha} - V_{load}^{1/\alpha}}{V_{sky}^{1/\alpha} - V_{load}^{1/\alpha}} \right) (T_{sky} - T_{load} - Offset) \quad (9)$$

To have an estimate of T_{ND} it is necessary to acquire an independent T_{sky} value. This is achieved through frequent tip curves. In the tip curve procedure, the opacity (τ) computed at each elevation angle is plotted as a function of airmass, and the slope of the regression (τ_z) is computed. T_{sky} is then determined as:

$$T_{sky} = T_b e^{-\tau} + T_{mr} (1 - e^{-\tau}) \quad (10)$$

where T_{mr} is the atmospheric mean radiating temperature. This T_{sky} value is then substituted in (9) to determine the *instantaneous* value of T_{nd} . Instantaneous values of T_{nd} are collected and stored. Once a day

the algorithm processes the acquired tip curves and determines a median value that is used in (6) and (8). An example of estimated T_{ND} for the 89 GHz channel is shown in Figure 5 (from [1]).

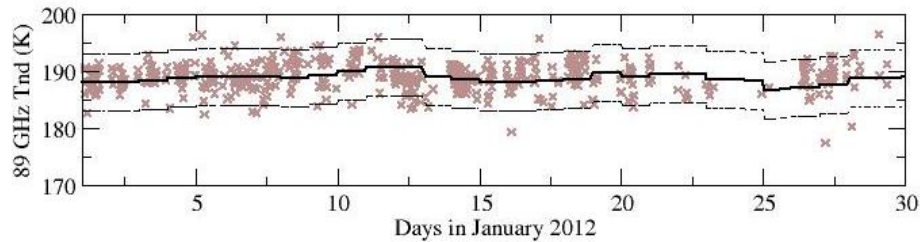


Figure 5. Instantaneous T_{nd} values derived from tip curves (brown points) and running median values (black line). The dashed lines represent two standard deviations from the mean.

7.3.3 History

2009–2011: Initial tests, design modification, and REM system development.

2011: Deployment of first three operational units at the AMF2, SGP, and TWP C3.

7.4 Operation and Maintenance

7.4.1 User Manual

User manuals are provided to the site operators during the deployment stage.

7.4.2 Routine and Corrective Maintenance Documentation

This section is not yet available.

7.4.3 Software Documentation

Documentation is available through the Data Management Facility or instrument mentor.

7.4.4 Additional Documentation

This section is not applicable to this instrument.

7.5 Glossary

Uncertainty: We define uncertainty as the range of probable maximum deviation of a measured value from the true value within a 95% confidence interval. Given a bias (mean) error B and uncorrelated random errors characterized by a variance σ^2 , the root-mean-square error (RMSE) is defined as the vector sum of these,

$$RMSE = (B^2 + \sigma^2)^{1/2}.$$

(B may be generalized to be the sum of the various contributors to the bias and σ^2 the sum of the variances of the contributors to the random errors). To determine the 95% confidence interval we use the Student's t distribution: $t_{n;0.025} \approx 2$, assuming the RMSE was computed for a reasonably large ensemble. Then the *uncertainty* is calculated as twice the RMSE.

8.0 References

[1] Cadeddu, MP, JC Liljegren, and DD Turner. “The Atmospheric Radiation Measurement (ARM) Program network of microwave radiometers: Instrumentation, data, and retrievals.” In preparation.

[2] MP Cadeddu, DD Turner, and JC Liljegren. 2009. “A neural network for real-time retrievals of PWV and LWP from arctic millimeter-wave ground-based observations.” *IEEE Transactions on Geoscience and Remote Sensing* 47(7):1887–1900.

[3] JC Liljegren. “Automatic self-calibration of ARM microwave radiometers,” in *Microwave Radiometry and Remote Sensing of the Earth's Surface and Atmosphere*. P Pampaloni and S Paloscia, Eds. Lorton, VA: VSP Book, 2000, pp. 433–443.



U.S. DEPARTMENT OF
ENERGY

Office of Science